Journal of Molecular Liquids 303 (2020) 112640

Contents lists available at ScienceDirect

Journal of Molecular Liquids

journal homepage: www.elsevier.com/locate/molliq

Effect of magnetic nanoparticles and silver-loaded magnetic nanoparticles on advanced wastewater treatment and disinfection

Aliasghar Najafpoor [a,b], Raziyeh Norouzian-Ostad [c], Hossein Alidadi [a,b], Tahereh Rohani-Bastami [d], Mojtaba Davoudi [a,b,*], Fateme Barjasteh-Askari [e,f,g], Jafar Zanganeh [h]

[a] Social Determinants of Health Research Center, Mashhad University of Medical Sciences, Mashhad, Iran
[b] Department of Environmental Health Engineering, School of Health, Mashhad University of Medical Sciences, Mashhad, Iran
[c] Department of Environmental Health Engineering, School of Health, Student Research Committee, Mashhad University of Medical Sciences, Mashhad, Iran
[d] Department of Chemical Engineering, Faculty of Engineering, Quchan University of Advanced Technology, Quchan, Iran
[e] Health Sciences Research Center, Torbat Heydariyeh University of Medical Sciences, Torbat Heydariyeh, Iran
[f] Department of Environmental Health, School of Health, Torbat Heydariyeh University of Medical Sciences, Torbat Heydariyeh, Iran
[g] Department of Environmental Health Engineering, School of Public Health, Tehran University of Medical Sciences, Tehran, Iran
[h] The Frontier Energy Centre, Chemical Engineering, School of Engineering, Faculty of Engineering & Built Environment, University of Newcastle, Callaghan, NSW 2308, Australia

ARTICLE INFO

Article history:
Received 21 July 2018
Received in revised form 26 January 2020
Accepted 2 February 2020
Available online 03 February 2020

Keywords:
Advanced wastewater treatment
Disinfection
Iron-oxide
Nanoparticles
Silver

ABSTRACT

Background: Strict discharge standards necessitate the advanced treatment and disinfection of wastewater treatment plant (WWTP) effluents for environmental protection and water reuse purposes. This study aimed to apply magnetic nanoparticles (MNPs) and silver-loaded magnetic nanoparticles (Ag-MNPs) in the advanced treatment and disinfection of the secondary effluent from a municipal WWTP.
Methods: The as-prepared nanoparticles were employed under various conditions of nanoparticle dose, contact time, and effluent contamination level. Total coliforms (TC), fecal coliforms (FC), heterotrophic bacteria (HB), and chemical oxygen demand (COD) were examined in the control and experimental samples to determine the treatment effectiveness.
Results: The findings showed that MNPs and Ag-MNPs were successfully synthesized with a mean size of 41 and 34 nm and the saturation magnetization of 62 and 67 emu/g, respectively. The results of advanced wastewater treatment showed that 105 mg/L nanoparticle dose, 70 min contact time, and 55% contamination level led to 0.65 TC, 0.48 FC, and 0.58 HB log reductions and 30.40% COD removal, on average. Increasing nanoparticle dose and contact time and decreasing contamination level enhanced the treatment efficacy. Switching from MNPs to Ag-MNPs significantly resulted in a 0.06 increase in TC, FC, and HB log reductions and a 6.16% increase in COD removal.
Conclusion: Based on the findings, MNPs and Ag-MNPs are promising in the advanced wastewater treatment and disinfection.

1. Introduction

The application of effluents from wastewater treatment plants (WWTPs) in agricultural and industrial purposes provides communities with numerous advantages including a low cost and sustained freshwater resource, compensation for treatment costs, reduction of the pressure on freshwater resources, and alleviation of the environmental impacts due to effluent discharge into water bodies [1]. Even when the direct reuse of effluents is not an option, it is still essential to monitor effluents discharged into the surface water and groundwater resources because they are largely used for drinking water supply [2]. In addition, in recent years, a new concern has emerged due to the presence of persistent organic pollutants (POPs) and trace heavy metals in water ecosystems. These compounds are toxic, carcinogenic, and mutagenic and can threaten the lives of human beings and animals [3,4]. Therefore, effluents from WWTPs must comply with environmental discharge standards and regulations that are being increasingly adopted stricter.

Total coliforms (TC) and fecal coliforms (FC) are common indicators of the microbiological quality of water bodies. Nowadays, the counting of heterotrophic bacteria (HB) by plate methods, however, is used as a complementary index to control water quality [5]. Residual organic matter is also another parameter used to examine the quality of WWTP effluents. The organic content of natural waters is typically expressed by chemical oxygen demand (COD). This chemical measure quantifies the extent of organic carbon based on milligrams of oxygen

* Corresponding author at: 18th Daneshgah Street, Mashhad, P.O. Box: 9137673119, Iran.
E-mail address: Davoudimj@mums.ac.ir (M. Davoudi).

https://doi.org/10.1016/j.molliq.2020.112640
0167-7322/

per liter of water. COD is a major parameter for measuring organic matter content, especially in the effluents from natural wastewater treatment systems.

The enhancement of the quality of secondary effluents before disinfection in WWTPs is achieved using advanced treatment technologies. Technologies such as adsorption, chemical coagulation, sand filtration, advanced oxidation, and membrane filtration are used to further decrease suspended solids, COD, nutrients, microbial load, and even dissolved solids. In recent decades, much attention has been paid to the application of nanoparticles in environmental purposes. This is because nanosized materials have a large surface area-to-mass ratio and high reactivity [6,7]. Thanks to these features, nanoparticles (NPs) have been widely used as catalysts [8], adsorbents [9,10], detectors [11], and disinfectants [12] in various studies. Due to their non-specific action, NPs as adsorbents are capable of removing a wide variety of contaminants including organics, inorganics, and colloids such as bacterial cells. When making a decrease in microbial contamination is a major goal, one can use some NPs with inherent disinfection capabilities such as magnetic nanoparticles [13]. Therefore, the need for adding other disinfectants such as chlorine and ozone, which are associated with adverse side effects, may be eliminated.

Magnetite (Fe_3O_4) is the strongest magnetic species among the transient metal oxides [14]. The reactive surface of iron-oxides allows for the adsorption of various impurities from water environment [15]. When used as NPs, called MNPs, they release reactive oxygen species (ROS) such as superoxide radicals (O_2^-), hydroxyl radicals ($^{\bullet}OH$), hydrogen peroxide (H_2O_2), and singlet oxygen ($^1O_2$) that can decompose proteins and DNA in bacterial cells [16]. Therefore, MNPs can exert their antibacterial effects through both physical adsorption and chemical disinfection. The magnetic feature of MNPs gives them an excellent separation property in the vicinity of an external magnetic field, which is essential for the removal of small-sized NPs from the effluent.

Silver (Ag) is a noble metal that exhibits a relatively weak oxidation behavior [17]. In large sizes, it is a low-reactive metal. However, in nanoscales, its microbicidal characteristic extremely enhances due to the increased specific surface area [18]. Like MNPs, Ag-NPs can exhibit their antibacterial activity through ROS generation [19]. In addition, other mechanisms have been mentioned such as the interaction of Ag-NPs with surface structures of bacterial cells and the reaction of released Ag ions with sulfur and phosphorous of cell macromolecules [20]. Accordingly, Ag has been used successfully in previous studies as a bactericidal agent against Gram-negative bacteria, e.g., coliforms [21]. The easy separation of the magnetite product can facilitate the recovery of invaluable Ag particles. It has been stated that Ag in combination with MNPs can penetrate biofilms more easily than Ag alone does [18]. Therefore, Ag-MNPs can show enhanced characteristics for water and wastewater treatment purposes.

There are several assumptions for the interaction of Ag and MNPs. Petrov, Ivantsov [22] modified Fe_3O_4 nanoparticles with Ag and could detect Ag both around magnetite NPs and as separate particles in the structure of Ag-MNPs. They also showed that Ag ions replaced Fe^{3+} ions in the Fe_3O_4 lattice. Therefore, a combination of physical and chemical interactions can play a role in the connection of Ag to MNPs structure.

Various studies in the literature investigated the antibacterial effects of magnetic Fe_3O_4 NPs alone or in combination with Ag-NPs as shells. For example, Ghaseminezhad, Shojaosadati [20] took advantage of the anti-biofilm activity of the compounds against antibiotic-resistant bacterial species in vitro. Joshi, Pant [23] employed the composite successfully against *E. coli* using the zone inhibition method on culture plates. However, limited studies are available to compare the effectiveness of MNPs and Ag-decorated MNPs against bacterial cells in environmental applications. Moreover, the efficacy of the nanocomposite in the decrease of organic content of environmental samples would be interesting to determine. As far as we know, there is no similar study in the literature to investigate the application of MNPs and Ag-MNPs for advanced purification and disinfection of WWTP effluents. Therefore, this study aimed to examine the effectiveness of magnetic nanoparticles (MNPs) and silver-loaded magnetic nanoparticles (Ag-MNPs) in the removal of Total Coliforms (TC), Fecal Coliforms (FC), Heterotrophic Bacteria (HB), and Chemical Oxygen Demand (COD) from real WWTP effluents.

2. Materials and methods

2.1. Chemicals

Iron(II) chloride tetrahydrate ($FeCl_2.4H_2O$), ammonia (NH_3), Polyvinylpyrrolidone (PVP, $(C_6H_9NO)_n$), and ethanol (C_2H_6O) were purchased from Merck and silver nitrate ($AgNO_3$) from Sigma-Aldrich. Distilled water (DW) was used to prepare all solutions.

2.2. NPs synthesis

To prepare Ag-MNPs according to a previous study [23], 200 mg $FeCl_2.4H_2O$ was dissolved in 20 mL DW. Then, 1 mL ammonia solution and 10 mg PVP were added to the solution under a chemical hood and stirred for 45 min on a shaker. In the next step, 10 mL DW, 5 mL ethanol, and 10 mL $AgNO_3$ solution (5.88 mM) were added to obtain a blackish-brown solution. The solution was transferred to a Teflon autoclave inside a stainless steel vessel and placed in an oven at 130 °C. After 3 h heating, the black sediment was washed several times with water and ethanol and dried at 30 °C for 12 h. MNPs (pure Fe_3O_4 NPs) were synthesized using a similar method without the step of $AgNO_3$ addition.

2.3. NPs characterization

The morphology and size of NPs were determined using Transmission Electron Microscopy (TEM, CM120, Philips, Netherlands). The X-ray diffraction (XRD, X'pert pro-XRD MPD PANalytical) patterns of the nanocomposite were studied over the Bragg angle 2θ range of 5–90°. The magnetic property of MNPs and Ag-MNPs were determined using Vibrating Sample Magnetometer (VSM, model 7400, Lakeshore Company, USA).

2.4. Design of experiments

In this study, a central composite design (CCD) under response surface methodology (RSM) in Design Expert V 7 software was used to design the experiments and determine the effectiveness of the as-prepared NPs for the advanced treatment of WWTP effluents. In CCD, we first defined factors (independent variables or parameters) that were effective on the response(s). The factors in this study included three numeric variables (NPs dose, contact time, and effluent contamination level), and one categorical variable (NPs type). The effluent contamination level was defined as the dilution proportion of real WWTP effluent in DW. Each numeric variable took five levels coded as $-\alpha$, -1, 0, $+1$, and $+\alpha$ (in the increasing order) while the categorical variable was coded at the levels of -1 and $+1$. The factors and their levels are presented in Table 1.

In this study, four responses were defined to assess the effect of changes in the levels of independent variables on the behavior of the

Table 1
Factors and their levels in CCD.

Factors	Levels				
	$-\alpha$	-1	0	$+1$	$+\alpha$
(X_1) NPs dose (mg/L)	10	48.5	105	161.5	200
(X_2) Contact time (min)	20	40.3	70	99.7	120
(X_3) Contamination level (%)	10	28.2	55	81.8	100
(X_4) NPs type	–	MNPs	–	Ag-MNPs	–

system. The responses included three biological parameters, including the logarithmic reduction (log reduction) in the number of TC, FC, and HB, and one chemical parameter, including the percentage of COD removal. The biological parameters indicated the capability of NPs to disinfect the WWTP effluent while the chemical parameter was to determine the effectiveness of NPs for removing colloidal and dissolved matters.

2.5. Experimentations

In this study, the effluent from a municipal WWTP in Mashhad, the second-largest city in Iran, was used to prepare working solutions. The plant was designed to treat the municipal wastewater stream with a flow rate of 15,200 m^3/d. The plant utilized unit operations and unit processes including bar screening units, aerated lagoons, facultative lagoons, polishing lagoons, and disinfection units. The samples were collected from the treated effluent before the disinfection units. They were transported to the laboratory in an icebox and kept at 4 °C until use. The analysis showed that the mean ± SD of the given contaminants in the effluent was as follows: TC (5.77 ± 1.08)E4 CFU/mL, FC (1.24 ± 0.19)E4 CFU/mL, HB (8.61 ± 0.87)E4 CFU/mL, and COD (229.31 ± 36.57) mg/L.

To prepare working solutions, various dilutions of effluent in sterile DW were prepared to give the contamination levels ranging from 10 to 100%. After reaching the room temperature, a working solution was divided into three 200-mL portions in 250-mL bakers. Two bakers were used as the experimental containers to receive either MNPs or Ag-MNPs while the third baker remained intact as the control one. All the three containers were placed under a similar shaking condition. When the required contact time elapsed, the shaking stooped and the solid phase was easily separated using a magnet. Then, 15 mL samples from the supernatant were withdrawn and kept at 4 °C before analysis for TC, FC, HB, and residual COD.

2.6. Microbial and chemical analysis

The analyses were performed within 6 h after sample collection. A conventional pour plate method was used to enumerate bacterial cells according to APHA standard method 9215B [24]. For *E. coli* enumeration, a 1-mL aliquot from a standard dilution of the sample was poured to 9-cm plates and then, 10-mL liquefied CHROMagar™ ECC kept at 44–46 °C was added. After incubating for 24 h at 37 °C, blue colonies indicated FC. To enumerate TC growing as red colonies, the incubation was done at 30 °C. To quantify the growth of HB, the pour plate method was conducted using Plate Count Agar as the medium and the plates were incubated at 35 °C for 48 h. The accurate results were produced by plates with 30 to 300 colonies. For each sample, three separate plates were prepared and the number of colonies was calculated using the following equation [25]:

$$N = \frac{\sum_{i=0}^{3} C}{3d} \quad (1)$$

where, N is the number of colony forming units per milliliter (CFU/mL), C is the number of colonies in each triple plate, and d is the dilution factor. Log reductions were calculated using the following formula:

$$\log reduction = \log\frac{N_C}{N_E} \quad (2)$$

where N_C denotes N in controls and N_E is N in experiments. Accordingly, one log reduction denoted a 90% removal efficiency of bacterial cells.

COD measurements were carried out following APHA standard method 5220D [24]. In brief, a 2.5-mL sample solution was added to vials containing 1.5 mL digestion solution and 3.5 mL sulfuric acid reagent. The vials were heated for 2 h at 150 °C in a HACH COD reactor (Model 45600, USA). After cooling down to room temperature, the absorbance was read at the wavelength of 600 nm using a spectrophotometer apparatus (Milton Roy Spectronic 20, USA). The COD removal efficiency was calculated using the following equation:

$$\text{COD removal } (\%) = \frac{COD_C - COD_E}{COD_C} \times 100 \quad (3)$$

where COD_C and COD_E represent COD in controls and experiments, respectively.

3. Results and discussion

3.1. NPs characteristics

TEM images were recorded to examine the morphologies of MNPs and Ag-MNPs and determine the particle sizes. TEM images are presented in Fig. 1. As can be observed, MNPs and Ag-MNPs were almost semi-spherical in shape. The TEM image of Ag-MNPs appeared darker than that of MNPs. It is also shown that our method of NPs synthesis could not produce uniform particles in size. The size of magnetic nanoparticles is dependent on various factors including synthesis conditions (e.g. oxygen-free environment) [26], pH of the synthesis medium [27], the ratio of base to iron ions, and the length of the alkyl chain R [28]. The mean diameter of particles in our study was 41 and 34 nm for MNPs and Ag-MNPs, respectively. The reduced size of particles by adding decorating agents has been also observed in the study by Joshi, Pant [23]. They used the same method of NPs synthesis as in our study and reported a reduced diameter from 26 to 20 nm after decorating MNPs with Ag. It seems that a decrease in the amount of iron-oxide precursor per unit volume of the preparation solution might be a reason for the reduced particle size in Ag-MNPs. However, there are reports in the literature [29] showing that the diameter of NPs increases when Ag shells decorated Fe_3O_4 cores. We believe that the procedure of nanoparticle synthesis has a major contribution to the characteristics of the nanocomposites including the particle size.

The particle sizes measured in this study conform to the findings of Naqvi, Samim [30] study, reporting the mean size of superparamagnetic iron oxide nanoparticles as 30 nm, and the findings of Ebrahimi, Rasoul-Amini [31] study, producing Fe_3O_4-Ag nanoparticles in the range of 23 to 54 nm. The latter study showed that the particle size is dependent on reducing agents used in the synthesis process. Santoyo Salazar, Perez [28] conducted a study on MNPs in the range of 10–40 nm and showed that nanoparticles of smaller than 20 nm had poor magnetic properties.

Fig. 2 represents the results of X-ray diffraction analysis of as-prepared nanocomposites. The characterization peaks were observed at 2θ values of 30.1°, 35.5°, 43.1°, 53.2°, 56.8°, and 62.3°, implying pure Fe_3O_4 in the MNPs structure. These values are in complete agreement with the values reported by Ebrahimi, Rasoul-Amini [31] and attribute to the indices (220), (311), (400), (422), (511), and (440) for Fe_3O_4 arises, respectively. The XRD patterns of Ag-MNPs showed the 2θ values of 38.1°, 44.3°, 64.2°, 77.6°, and 81.5° corresponding to the (111), (200), (220), (311), and (222) planes of cubic Ag, respectively.

The VSM analysis was conducted to determine the magnetic properties of NPs, and the results are presented in Fig. 3. Typical superparamagnetic behavior is observed for both MNPs and Ag-MNPs due to the absence of any remanence or coercivity. The analysis showed the saturation magnetization (Ms) values of 62 and 67 emu/g for MNPs and Ag-MNPs, respectively. The increasing Ms. values in the nanocomposite might have been due to the interactions between the nanoparticles that changed the anisotropic energy. There are conflicting results in the literature regarding the VSM analysis of Fe_3O_4-Ag core-shell structures. For example, Liu, Zhou [29], in line with our study, reported an increase in the Ms. values when Ag was doped on the surface of iron-oxide NPs, while Li, Yue [32] and Ghaseminezhad and Shojaosadati [18]

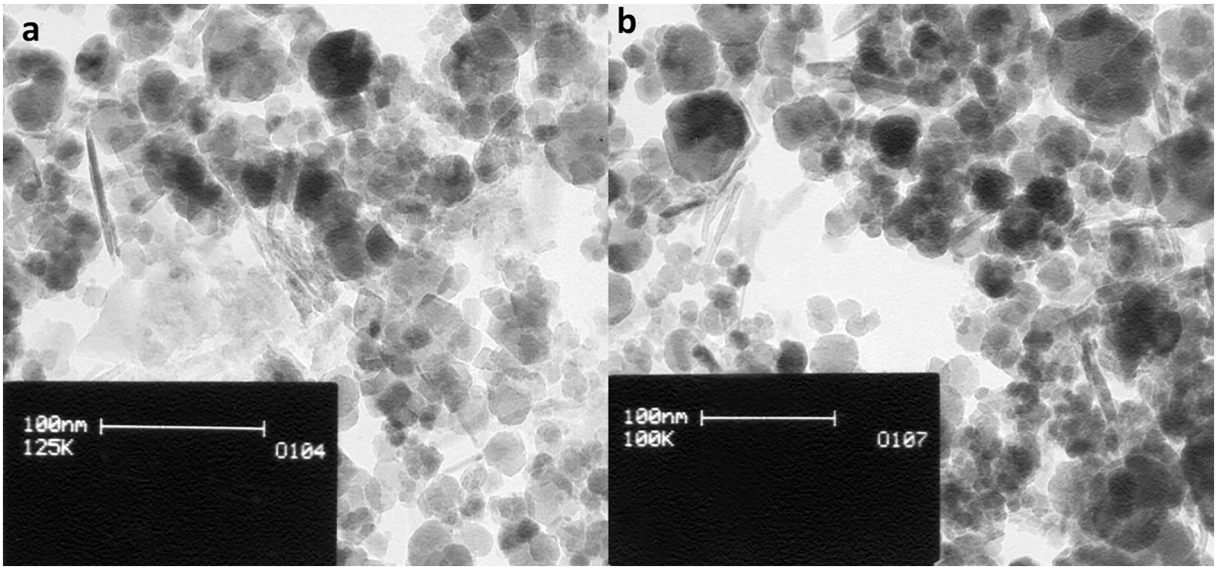

Fig. 1. TEM images of MNPs (a) and Ag-MNPs (b).

demonstrated antagonist results. It seems we need a comprehensive study to gain further insight into changes in the magnetic properties of iron-oxide nanocomposites as a function of doping agents to make a general conclusion.

3.2. Treatment of WWTP effluent

The detailed experimental results of WWTP effluent advanced treatment using MNPs and Ag-MNPs are presented in Table S1 (see supplementary material). Table 2 summarizes the values of descriptive statistics including mean, standard deviation, minimum and maximum removal efficiencies separately for contaminants and nanoparticles. The number of observations was 20 for each set of experiments.

As can be seen, Ag-MNPs were more efficient than MNPs in the removal of all contaminants including TC, FC, HB, and COD from the WWTP effluent. The obtained data were analyzed by the analysis of variance (ANOVA) to develop the best models describing the experimental conditions. The developed models are as follows:

$$Y_1 = 0.65 + 0.094X_1 + 0.054X_2 - 0.086X_3 + 0.031X_4 \quad (4)$$

$$Y_2 = 0.48 + 0.044X_1 + 0.035X_2 - 0.066X_3 + 0.032X_4 \quad (5)$$

$$Y_3 = 0.58 + 0.078X_1 + 0.043X_2 - 0.078X_3 + 0.032X_4 \quad (6)$$

$$Y_4 = 30.40 + 7.68X_1 + 1.33X_2 - 8.79X_3 + 3.08X_4 \quad (7)$$

In these equations, Y_1, Y_2, Y_3, and Y_4 denote TC log reduction, FC log reduction, HB log reduction, and COD removal (%), respectively. X_1 to X_4 represent NPs dose, contact time, contamination level, and NPs type, respectively. Eqs. (4) to (7) show that the treatment process could lead to TC, FC, and HB reductions as 0.65, 0.48, and 0.88, respectively, in log units and COD as 30.40%, irrespective of changes at the levels of the parameters.

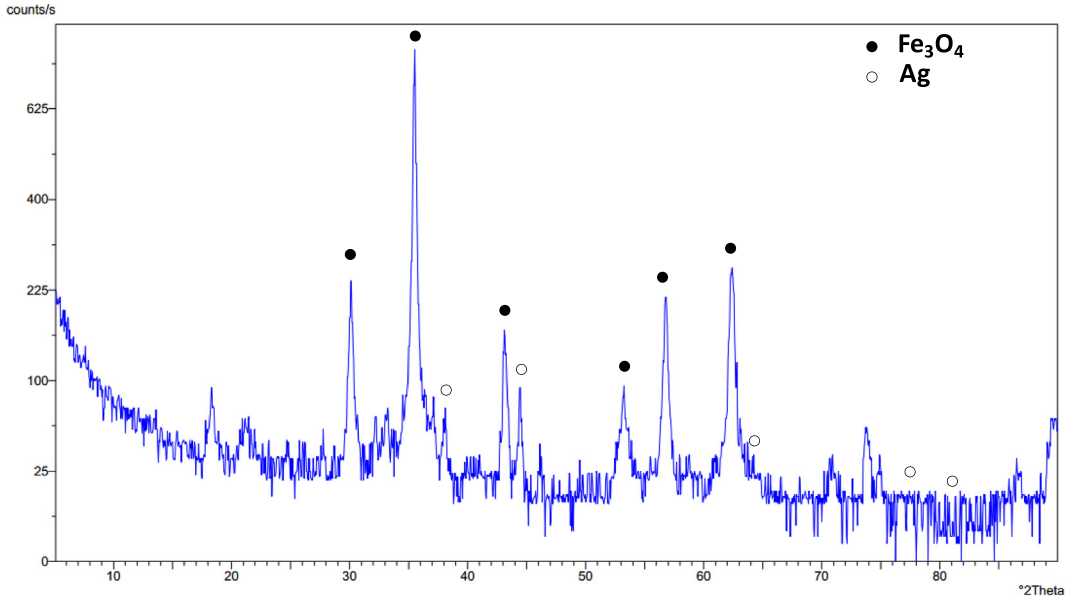

Fig. 2. The XRD pattern of the nanocomposite containing Fe_3O_4 and Ag.

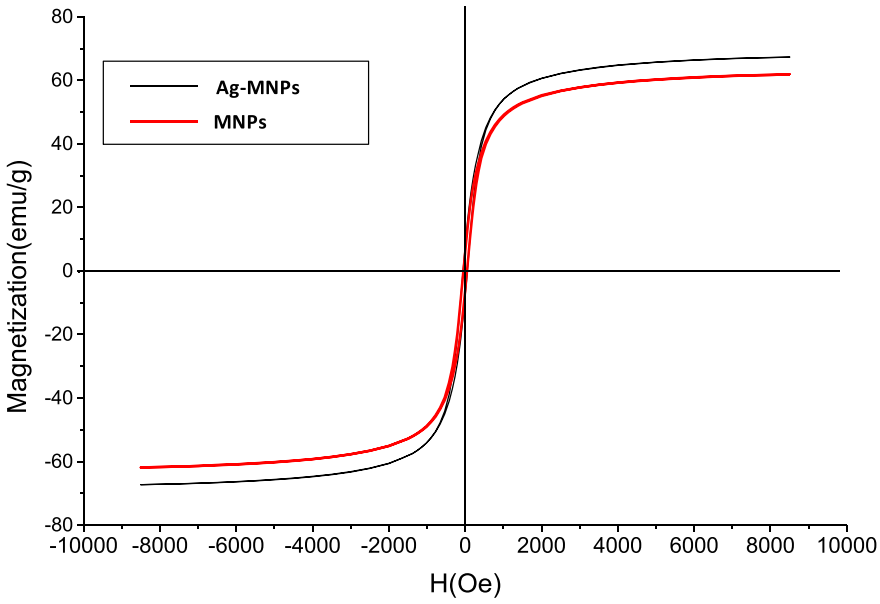

Fig. 3. Magnetic hysteresis loops of MNPs and Ag-MNPs at room temperature.

The statistical analysis (Table S2) showed that all the models were statistically significant at the significance level of 95%. Moreover, it was disclosed that all the parameters (X_1 to X_4) could significantly affect the responses (Y_1 to Y_4) (p-values<0.05). The only exception was the effect of contact time (X_2) on the percentage of COD removal that was insignificant (p-value = 0.17). Table 3 summarizes the results of data fitting to the models. The R^2 values are used to explore the correlation of experimental data with the predicted ones. According to Table 3, only 28.66%, 24.48%, 20.81%, and 17.49% of the total variance could not be explained by Y_1, Y_2, Y_3, and Y_4 models, respectively. The Adj. R^2 is a parameter used to correct the R^2 values for sample size and number of terms included in the models. Pred. R^2 measures the amount of variation when a new set of data are explained by the model. A difference of ≤0.2 between Adj. R^2 and Pred. R^2 indicates the goodness of the fit of the model. This condition was well satisfied with the developed models, as observed in Table 3. Adequate precision is a parameter measuring the signal-to-noise ratio. The values of >4 are desirable. These values were in the range of 18.65 to 23.56 for Y_1 to Y_4 models, indicating quite acceptable signal-to-noise ratios.

3.3. Effect of parameters

We examined the effect of four parameters including NPs dose, contact time, contamination level, and NPs type on the removal of four contaminants including TC, FC, HB, and COD from the WWTP effluent. As mentioned earlier, all the parameters had significant effects on the responses.

3.3.1. NPs dose

It has been well established that increasing nanoparticle dose in a specific range increases the removal efficiency of the target contaminant [33,34]. This behavior was also observed in the current study. An increase in MNPs doses from 48.5 to 161.5 mg/L led to increased log reduction of TC from 0.52 to 0.71, FC from 0.40 to 0.49, and HB from 0.47 to 0.62, as well as increased COD removal from 19.65 to 35.00%. In the presence of Ag-MNPs, the increased dose at the same levels could increase the TC, FC, and HB log reductions respectively from 0.58 to 0.77, from 0.47 to 0.56, and from 0.53 to 0.69, and COD removal from 25.80 to 41.15%. Joshi, Pant [23] showed a dose-dependent behavior for the 4-nitrophenol reduction in the presence of Ag-iron oxide/reduced graphene oxide nanocomposite as the adsorbent. The accumulation of Ag-NPs on the cell wall of the bacteria and the penetration into the cell are considered the causes of bacterial death. By increasing the concentration of NPs, more ions are released and penetrate the cell [35]. In addition, by increasing the dose of NPs, the surface required for adsorbing contaminants increases and ultimately the removal efficiency improves. However, it should be noted that an excessive increase in nanoparticle doses not only could not be cost-effective, but also may cause nanoparticles to agglomerate and, by forming larger particles, ultimately reduce the adsorbent effective surface.

3.3.2. Contact time

In the current study, increasing contact time from 40.3 to 99.7 min could significantly increase TC log reduction from 0.56 to 0.67, FC log reduction from 0.41 to 0.48, and HB log reduction from 0.55 to 0.59 when MNPs were used as the adsorbent. In the presence of Ag-MNPs, an increase in contact time at the same levels resulted in an increased log reduction for TC from 0.62 to 0.73, FC from 0.48 to 0.55, and HB from 0.57 to 0.65. In the case of COD removal, although increasing contact time cloud improve removal efficiencies (from 26.00 to 28.66% for MNPs and from 32.14 to 34.81 for Ag-MNPs), the increases were statistically

Table 2
A summary of the experimental results of real effluent treatment using MNPs and Ag-MNPs.

Response	Units	MNPs				Ag-MNPs			
		Min	Max	Mean	SD	Min	Max	Mean	SD
TC reduction	Log reduction	0.42	0.92	0.62	0.13	0.46	1.04	0.68	0.15
FC reduction	Log reduction	0.32	0.62	0.45	0.07	0.35	0.70	0.51	0.09
HB reduction	Log reduction	0.38	0.80	0.55	0.10	0.41	0.85	0.61	0.12
COD removal	Removal percentage	11.78	45.82	27.32	10.28	15.71	52.86	33.47	11.26

Table 3
The regression results of the developed models.

Model	R^2	Adj. R^2	Pred. R^2	Adequate precision
Y_1	0.7134	0.6806	0.6012	18.65
Y_2	0.7552	0.7272	0.6633	20.95
Y_3	0.7919	0.7682	0.7104	23.15
Y_4	0.8251	0.8051	0.7777	23.56

insignificant. This indicates that the effective range of contact time was different for the removal of COD and reduction of bacterial cells in this study.

3.3.3. Contamination level

In the current study, the level of contamination was adjusted by pouring various amounts of WWTP effluent into distilled water to reach a pollution level from 10 to 100%. The obtained results showed that the contamination level within the aforementioned range had statistically significant effects on all responses. In the presence of MNPs, increasing the contamination level from 28.2 to 81.8% reduced TC log reduction from 0.70 to 0.53, FC log reduction from 0.51 to 0.38, HB log reduction from 0.62 to 0.47, and COD removal from 36.12 to 18.53%. In the presence of Ag-MNPs, when the contamination level increased from 28.2 to 81.8%, TC, FC, and HB log reduction rates decreased respectively from 0.76 to 0.59, from 0.58 to 0.45, and from 0.69 to 0.53, and COD removal from 42.27 to 24.68%. As observed in many previous studies, when the initial load of contaminants increases, the removal efficiency decreases at a fixed dose of NPs as remediating agents, whether chemical disinfection is the mechanism of action or simple physical adsorption. Sondi and Salopek-Sondi [35] showed that increasing the bacterial load from 10^4 to 2×10^5 increases the number of *E. coli* viable cells from 0 to about 400 CFU in each plate.

3.3.4. NPs type

MNPs and Ag-MNPs have served as remediating agents in various studies because of their bactericidal and antifungal effects. It has been proven that MNPs can release reactive oxygen species (ROS), contributing to the disinfection of water environment [16]. The antibacterial activity of Ag-MNPs with the shell-core structure is attributed to Ag ions slowly released from the nanoparticle surface into the solution [36]. In addition, both MNPS and Ag-MNPs inherently are nanostructured adsorbents for bacterial cells, as well as for other contaminants including organic matter. Therefore, the separation of the mass of the adsorbent from bulk solution leads to the water disinfection and COD reduction simultaneously.

However, in this study, that MNPs or Ag-MNPs were used for the effluent treatment made a significant difference in the outcomes. The results showed that switching from MNPs to Ag-MNPs could result in a 0.06 increase in TC, FC, and HB log reductions and a 6.16% increase in the removal rate of COD. Although the magnitudes of the increases may seem negligible technically, they were significant statistically. It seems that Ag NPs decorating the surface of iron-oxide NPs exerted an extra antibacterial effect. This finding is in agreement with the results of a study conducted by Amarjargal, Tijing [37] showing that the antibacterial effect of Ag-Fe_3O_4 nano-composites was much higher than the effect of Fe_3O_4 nanoparticles against *E. coli*. They also reported that increasing silver concentration in the precursor solution used to prepare Ag-MNPs improved the antibacterial activity of the nanocomposite remarkably. Ghaseminezhad and Shojaosadati [18] disclosed that the bactericidal activity of Ag-MNPs was dependent on the size of silver particles in the composite, as well.

Another observation in our study was the enhanced removal of COD in the presence of Ag-MNPs rather than MNPs. This may be due to the smaller size of Ag-MNPs that provided more surface area per unit mass of NPs for the adsorption of organic matter in the solution. Unlike MNPs that have been well studied for the removal of organic pollutants, Ag-doped and Ag-based adsorbents have been rarely used for the removal of contaminants other than pathogens. Srilakshmi and Saraf [38] conducted a study to adsorb Congo red dye onto Ag-doped hydroxyapatite. They showed that the removal efficiency of dye increased with increasing the amount of Ag doped onto hydroxyapatite particles, which was attributed to the higher surface area and expanded pore volume of the adsorbent. In another study, Satapathy and Das [39] showed that soil particles doped with Ag NPs were more efficient adsorbents than uncoated soil particles for the removal of crystal violet dye.

3.4. Strengths and limitations

Using real WWTP effluents to prepare working solutions and employing a control sample in each set of the experiments to be compared with the experimental samples strengthened the current study. However, there were some limitations including that the study was not designed to distinguish the role of physical adsorption and chemical disinfection in the removal of bacterial cells. In addition, the synergistic effect of MNPs and Ag-MNPs was not investigated.

4. Conclusion

The study showed that doping Ag ions onto Fe_3O_4 nanoparticles reduces the particle size and increases the magnetic properties of the as-prepared nanocomposites. Ag-MNPs also exhibited significantly higher efficacy for effluent disinfection (by increasing the log reduction of TC, FC, and HB) and advanced treatment (by increasing the removal of COD). Therefore, it is suggested that Ag-MNPs be considered as an alternative in the advanced treatment and disinfection of effluents in wastewater treatment plants.

Funding

This project was supported by the Research Deputy of Mashhad University of Medical Sciences, Mashhad, Iran (Project No. 931173).

CRediT authorship contribution statement

Aliasghar Najafpoor: Conceptualization, Methodology, Supervision, Validation. **Raziyeh Norouzian Ostad:** Conceptualization, Methodology, Investigation, Writing the original draft. **Hossein Alidadi:** Supervision, Validation. **Tahereh Rohani-Bastami:** Data curation, Formal analysis, Supervision, Validation. **Mojtaba Davoudi:** Conceptualization, Methodology, Investigation, Writing, review & editing. **Fateme Barjasteh-Askari:** Data curation, Formal analysis, Writing the original draft. **Jafar Zanganeh:** Writing, review & editing.

Declaration of competing interest

The authors declare that there is no conflict of interest associated with this manuscript.

Appendix A. Supplementary data

Supplementary data to this article can be found online at https://doi.org/10.1016/j.molliq.2020.112640.

References

[1] B. Hodgson, et al., Impact of water conservation and reuse on water systems and receiving water body quality, Environ. Eng. Sci. 35 (6) (2017) 545–559.
[2] A. Najafpoor, et al., Quality assessment of the Kashaf river in north east of Iran in 1996-2005, J. Appl. Sci. 7 (2) (2007) 253–257.
[3] S. Garcia-Segura, J.D. Ocon, M.N. Chong, Electrochemical oxidation remediation of real wastewater effluents — a review, Process Saf. Environ. Prot. 113 (2018) 48–67.
[4] A.R. Rahmani, et al., Adsorption of lead metal from aqueous solutions using activated carbon derived from scrap tires, Fresenius Environ. Bull. 24 (7) (2015) 2341–2347.

[5] S. Golbaz, et al., An innovative swimming pool water quality index (SPWQI) to monitor and evaluate the pools: design and compilation of computational model, Environ. Monit. Assess. 191 (7) (2019) 448.
[6] S. Wu, et al., Identification and quantification of titanium nanoparticles in surface water: a case study in Lake Taihu, China, J. Hazard. Mater. (2019) 121045.
[7] L. Qin, et al., "Gold rush" in modern science: fabrication strategies and typical advanced applications of gold nanoparticles in sensing, Coord. Chem. Rev. 359 (2018) 1–31.
[8] C.-J. Zhong, M.M. Maye, Core–shell assembled nanoparticles as catalysts, Adv. Mater. 13 (19) (2001) 1507–1511.
[9] H. Sadegh, et al., The role of nanomaterials as effective adsorbents and their applications in wastewater treatment, J. Nanostruct. Chem. 7 (1) (2017) 1–14.
[10] X. Zhou, et al., Preparation of water-compatible molecularly imprinted thiol-functionalized activated titanium dioxide: selective adsorption and efficient photodegradation of 2, 4-dinitrophenol in aqueous solution, J. Hazard. Mater. 346 (2018) 113–123.
[11] C. Lai, et al., Chitosan-wrapped gold nanoparticles for hydrogen-bonding recognition and colorimetric determination of the antibiotic kanamycin, Microchim. Acta 184 (7) (2017) 2097–2105.
[12] S.R. Shaffiey, S.F. Shaffiey, Silver oxide–copper oxide nanocomposite preparation and antimicrobial activity as a source for the treatment of fish diseases: silver oxide–copper oxide Nanocomposite preparation and antimicrobial activity, Advancing Medicine Through Nanotechnology and Nanomechanics Applications, IGI Global 2017, pp. 140–151.
[13] X. Zhang, et al., Loading Cu-doped magnesium oxide onto surface of magnetic nanoparticles to prepare magnetic disinfectant with enhanced antibacterial activity, Colloids Surf. B: Biointerfaces 161 (2018) 433–441.
[14] I. Ali, et al., Phytogenic magnetic nanoparticles for wastewater treatment: a review, RSC Adv. 7 (64) (2017) 40158–40178.
[15] H. Daraei, A. Amrane, H. Kamali, Assessment of phenol removal efficiency by synthesized zero iron nanoparticles and Fe powder using the response surface methodology, Iran. J. Chem. Chemi. Eng. (IJCCE) 36 (3) (2017) 137–146.
[16] N. Tran, et al., Bactericidal effect of iron oxide nanoparticles on Staphylococcus aureus, Int. J. Nanomedicine 5 (2010) 277.
[17] C. Sachse, et al., ITO-free, small-molecule organic solar cells on spray-coated copper-nanowire-based transparent electrodes, Adv. Energy Mater. 4 (2) (2014), 1300737.
[18] S.M. Ghaseminezhad, S.A. Shojaosadati, Evaluation of the antibacterial activity of Ag/Fe3O4 nanocomposites synthesized using starch, Carbohydr. Polym. 144 (2016) 454–463.
[19] M.I. Azócar, et al., Capping of silver nanoparticles by anti-inflammatory ligands: antibacterial activity and superoxide anion generation, J. Photochem. Photobiol. B Biol. 193 (2019) 100–108.
[20] S.M. Ghaseminezhad, S.A. Shojaosadati, R.L. Meyer, Ag/Fe3O4 nanocomposites penetrate and eradicate S. aureus biofilm in an in vitro chronic wound model, Colloids Surf. B: Biointerfaces 163 (2018) 192–200.
[21] M. Davoudi, et al., Antibacterial effects of hydrogen peroxide and silver composition on selected pathogenic enterobacteriaceae, Int. J. Environ. Health Eng. 1 (1) (2012) 23.
[22] D. Petrov, et al., Magnetic and magneto-optical properties of Fe3O4 nanoparticles modified with Ag, J. Magn. Magn. Mater. 493 (2020), 165692.
[23] M.K. Joshi, et al., One-pot synthesis of Ag-iron oxide/reduced graphene oxide nanocomposite via hydrothermal treatment, Colloids Surf. A Physicochem. Eng. Asp. 446 (2014) 102–108.
[24] Federation, W.E, A.P.H. Association, Standard Methods for the Examination of Water and Wastewater, American Public Health Association (APHA), Washington, DC, USA, 2005.
[25] E. Babaei, et al., A study on inhibitory effects of titanium dioxide nanoparticles and its photocatalytic type on Staphylococcus aureus, Escherichia coli and Aspergillus flavus, Appl. Food Biotechnol. 3 (2) (2016) 115–123.
[26] A.K. Gupta, A.S. Curtis, Lactoferrin and ceruloplasmin derivatized superparamagnetic iron oxide nanoparticles for targeting cell surface receptors, Biomaterials 25 (15) (2004) 3029–3040.
[27] A. Petri-Fink, et al., Development of functionalized superparamagnetic iron oxide nanoparticles for interaction with human cancer cells, Biomaterials 26 (15) (2005) 2685–2694.
[28] J. Santoyo Salazar, et al., Magnetic iron oxide nanoparticles in 10— 40 nm range: composition in terms of magnetite/maghemite ratio and effect on the magnetic properties, Chem. Mater. 23 (6) (2011) 1379–1386.
[29] C. Liu, et al., Preparation and characterization of Fe3O4/Ag composite magnetic nanoparticles, Inorg. Mater. 44 (3) (2008) 291–295.
[30] S. Naqvi, et al., Concentration-dependent toxicity of iron oxide nanoparticles mediated by increased oxidative stress, Int. J. Nanomedicine 5 (2010) 983.
[31] N. Ebrahimi, et al., Comparative study on characteristics and cytotoxicity of bifunctional magnetic-silver nanostructures: synthesized using three different reducing agents, Acta Metall. Sin. (English Lett.) 29 (4) (2016) 326–334.
[32] W. Li, et al., Synthesis and characterization of magnetically recyclable Ag nanoparticles immobilized on Fe3O4@ C nanospheres with catalytic activity, Appl. Surf. Sci. 335 (2015) 23–28.
[33] I. Ali, C. Peng, I. Naz, Removal of lead and cadmium ions by single and binary systems using phytogenic magnetic nanoparticles functionalized by 3-marcaptopropanic acid, Chin. J. Chem. Eng. 27 (4) (2019) 949–964.
[34] I. Ali, et al., Green synthesis of phytogenic magnetic nanoparticles and their applications in the adsorptive removal of crystal violet from aqueous solution, Arab. J. Sci. Eng. 43 (11) (2018) 6245–6259.
[35] I. Sondi, B. Salopek-Sondi, Silver nanoparticles as antimicrobial agent: a case study on E. coli as a model for Gram-negative bacteria, J. Colloid Interface Sci. 275 (1) (2004) 177–182.
[36] A. Amarjargal, et al., Simultaneous synthesis of TiO2 microrods in situ decorated with Ag nanoparticles and their bactericidal efficiency, Curr. Appl. Phys. 12 (4) (2012) 1106–1112.
[37] A. Amarjargal, et al., Simultaneous preparation of Ag/Fe3O4 core–shell nanocomposites with enhanced magnetic moment and strong antibacterial and catalytic properties, Chem. Eng. J. 226 (2013) 243–254.
[38] C. Srilakshmi, R. Saraf, Ag-doped hydroxyapatite as efficient adsorbent for removal of Congo red dye from aqueous solution: synthesis, kinetic and equilibrium adsorption isotherm analysis, Microporous Mesoporous Mater. 219 (2016) 134–144.
[39] M.K. Satapathy, P. Das, Optimization of crystal violet dye removal using novel soil-silver nanocomposite as nanoadsorbent using response surface methodology, J. Environ. Chem. Eng. 2 (1) (2014) 708–714.